Article

Technical and Eco-Efficiency Implications of the Use of Basalt Fibre in Hybrid Composites

Chensong Dong, Garreth Howie, Rafael Costelo and Wahidul Biswas *

School of Civil and Mechanical Engineering, Curtin University, Perth, WA 6845, Australia; C.Dong@curtin.edu.au (C.D.); g.howie@student.curtin.edu.au (G.H.); rafael.costelo@graduate.curtin.edu.au (R.C.)

* Corresponding author. E-mail: w.biswas@curtin.edu.au (W.B.)

ABSTRACT: The use of hybrid composites can be environmentally friendlier than the traditional materials since renewable resources, both natural and synthetic fibres can be incorporated into the composites, resulting in lighter weight, enhanced resource efficiency, durability, and biodegradability, which could potentially make them sustainable materials for structural applications. Basalt fibre being treated with hydrochloric acid exhibits superior adhesion with the epoxy matrix, improving overall strength and stiffness. Thus, the aim of this paper is to determine the eco-efficiency of two types of hybrid composites: glass/basalt and carbon/basalt fibre-reinforced under flexural loading. The flexural strengths of these composites were obtained through a Finite Element Analysis (FEA) model using Ansys workbench. These simulation-based flexural strengths form the basis for the quadratic regression model to establish a relationship between the different flexural strengths and fibre volume fractions combinations. Given the required flexural strength between 900 and 1300 MPa, the optimal candidates/layups were identified with the aid of the model. An environmental study following a life cycle assessment (LCA) and eco-efficiency framework of unidirectional glass/basalt and carbon/basalt fibre-reinforced hybrid composites with varying fibre volume fractions is presented in this paper to select the eco-efficient composites. In the case of glass/basalt fibre-reinforced hybrid composites, the designs with the highest eco-efficiency for 900 and 1200 MPa are $[BG_3]_S$ with more glass fibre and $[G_7B]$ with more glass fibre, respectively, due to having lower costs and environmental impacts. For carbon/basalt fibre-reinforced composites, the stacking sequence $[B_8]$ was deemed to be the most eco-efficient. Finally, epoxy has the highest economic and environmental cost. Therefore, composite designs with high glass fibre content are considered eco-efficient since they have a lower epoxy content.

Keywords: Basalt; Glass; Carbon; Hybrid composites; Flexural strength; Eco-efficiency

1. Introduction

Hybrid composites are materials made by combining two or more different types of fibres within a single matrix. These fibres can be of different materials, such as carbon, glass, basalt, aramid, or natural fibres. The goal of creating hybrid composites is to leverage the unique properties of each fibre type to achieve a material with enhanced overall performance. By combining different fibres, hybrid composites can be engineered to exhibit specific mechanical, thermal, and chemical properties that are superior to those of single-fibre composites. Hybrid composites often show improved strength, stiffness, and toughness, making them suitable for demanding applications. Using a combination of fibres can reduce the overall cost of the composite material, especially when expensive fibres like carbon are partially replaced with more affordable ones like glass or basalt.

Hybrid composites have gained significant attention in materials science due to their versatile applications and potential benefits. The combination of different fibres can result in composites with superior mechanical properties, such as higher tensile strength, impact resistance, and fatigue life. This makes them ideal for use in aerospace, automotive, and construction industries [1]. Hybrid composites can contribute to sustainability by incorporating natural fibres or recycled materials, reducing the environmental impact of composite production [2]. In applications where weight is a critical factor, such as in the aerospace and automotive industries, hybrid composites can offer a lightweight alternative to traditional materials without compromising strength and durability [3]. The ability to tailor the properties

of hybrid composites allows for greater design flexibility, enabling engineers to create materials that meet specific performance requirements for various applications.

Aramid fibres, such as Kevlar, have a high tensile strength (2800–4100 MPa), but they are not a popular material for structural engineering due to their high production cost, relatively low compressive strength (500–1000 MPa), and hygroscopic tendency [4]. Recently, much interest has been given to using natural fibres such as flax, hemp, grass, and cotton for reinforcement of composite materials as their inclusion can reduce the economic and environmental cost of producing the material. Although several studies have shown promising results [4–6], the mechanical properties of natural fibres remain inadequate for structural applications, and there is a lack of long-term performance data that limits their application [6]. By optimizing the use of different fibres, hybrid composites can provide a cost-effective solution for high-performance applications, balancing performance and affordability.

Basalt fibres are an environmentally friendly option when compared to other FRPs such as GFRP (glass fibre-reinforced polymer), and CFRP (carbon fibre-reinforced polymer) as the energy consumption during processing is less intensive and the absence of additional chemicals needed during processing provides an eco-friendly product. Basalt is nontoxic and considered safe for human exposure, even as powdered particles [7,8].

Basalt fibre has a relatively higher tensile, and compressive strength as well as a higher Young's modulus when compared to glass fibre [8–11]. Basalt fibres can withstand environments of up to 700 °C [12] while maintaining structural integrity, with the fibre only melting at 1450 °C [13]. Research conducted by Adulrhaman et al. [9] indicates that BFRP is a topic of interest in the oil and gas sector due to the chemical resistance and improved lifespan of polymer composite pipes. It was also found that the refurbishment of old mining vessels using composite parts can save upwards of 700 tons of mass that does not need to be transported [9].

BFRP's are used in automotive, aerospace, sporting, and wind energy applications due to their specific strength, thermal and electrical properties [8].

Additionally, BF provides better mechanical, thermal properties and other beneficial characteristics, such as better fatigue life over GF, when applied in composites [14–16]. Unfortunately, the application of BF and its composites is still in its early stages. Due to a lack of real-world application data and lower production volume of BF compared to GF [17].

One of the benefits found for the carbon/glass fibre-reinforced hybrid composites is the improvement of flexural strength, which is noted as the positive hybrid effect. Similar positive hybrid effects were also found with the carbon/basalt fibre-reinforced hybrid composite [18]. Fiore et al. [19] showed that the highest improvement in the mechanical properties was achieved when two external glass mats were replaced by uniaxial basalt fabrics. Bozkurt [20] showed that higher improvements in the flexural properties of aramid composites were found with the introduction of basalt layers to the compressive side, compared to the introduction of basalt layers to the tensile side. For the glass/basalt and aramid/basalt hybrid composites, it was also shown that the sandwich-like structures offered the best flexural behaviour [21,22].

Pu et al. [23] explored the low-velocity impact properties and optimal hybrid ratio range for improving the properties of hybrid composites. The research highlights that placing basalt fibres on the compression side and increasing the proportion of carbon fibres can significantly enhance energy absorption capacity under low-velocity impact loads. The study also discusses the application of these hybrid composites in automobile engine hoods. Azimpour-Shishevan et al. [24] investigated the effects of intra-ply hybridization on the mechanical and thermal properties of carbon/basalt fibres-reinforced epoxy composites. The combination of carbon fibre's superior mechanical properties and basalt fibre's good thermal stability and toughness is the focus of this study. Kuciel et al. [25] evaluated the mechanical and thermal performance of hybrid bio-based poly (ethylene terephthalate) composites reinforced with basalt and carbon fibres using injection moulding. The presented work shows that the simultaneous addition of two types of fibres will positively affect the mechanical, thermal, and performance properties.

Fidan et al. [26] examine how erosive wear affects hybrid composites made by vacuum-infusing glass and basalt fibres into an epoxy matrix. The research finds that glass layers enhance erosion resistance, while basalt layers increase wear. The study emphasizes the strategic selection and layering of materials for enhanced durability. Balasubramanian et al. [27] assess the performance of hybrid composites reinforced with basalt and glass fibres under quasi-static indentation tests. The study finds that hybridization of glass fibres with basalt fibres results in superior load-bearing ability and better energy absorption characteristics compared to basalt/epoxy composites. Natarajan et al. [28] report that hybridization of basalt and glass fibres increases tensile strength and interlaminar shear strength. The research highlights the benefits of hybrid fillers over single fibres.

Raajeshkrishna et al. [29] used basalt/epoxy and glass/epoxy layers to fabricate sandwich-type laminated composites. These composites were tested with different surface treatments. It was found that the stacking sequence

and surface treatment of the fibres played an important role in improving the mechanical properties of the hybrid composite. The basalt fibres that have been treated with hydrochloric acid have superior adhesion with the epoxy matrix, improving overall strength and stiffness. The stacking sequence that showed the highest tensile strength was G5/B4/G5, with a strength of 356.39 MPa.

Whilst these composite materials offer better structural properties and could potentially improve environmental performance through enhanced durability, an eco-efficiency analysis is important as it will help select the composite materials without entailing excessive cost. Eco-efficiency considers both the economic and environmental costs of a manufacturing process and can be used to assist in cost-effectively reducing environmental impacts [30]. This paper aims to define a framework to assist in assessing the economic and ecological effects associated with manufacturing. The following framework has been adapted from work done by Arceo [30] and Jayawardane [31] and can be used to assess the economic and environmental efficiency of FRPs. Several research papers regarding eco-efficiency have followed this framework with great success [5,30,31]. The German chemical company BASF used a similar model for process selection in 2002 [32]. This framework relies upon Life Cycle Assessment (LCC) and Life Cycle Costing (LCC) to develop an eco-efficiency portfolio that gives a graphic representation of normalised cost and normalised ecological impacts [31]. Also, life cycle approaches can consider all life cycle stages for a decision in terms of achieving a circular economy, but the consideration of the whole life cycle is beyond the scope of the current work [33]. Some materials that can be recycled at their end of life are bioplastics, natural fibres, and some metals, oil-based plastics and chemicals so long as they are not mixed work [33].

The basis of this study is to assess the eco-efficiency performance of manufacturing glass/basalt fibre-reinforced hybrid composites in Australia. This investigation applies a framework for decision-making that can be used in selecting environmentally friendly designs. The steps taken in this study can be applied to other manufacturing processes and prove to be a useful guide for future research. The work compiled within this investigation aims to provide further insight into life cycle thinking and sustainable manufacturing. The hypothesis is to apply an eco-efficiency framework that assesses the cost and environmental implications of the use of different types of reinforcement fibres in different hybrid composite materials.

The primary purpose of this study is to conduct a comprehensive Life Cycle Assessment (LCA) of hybrid composites reinforced by carbon/basalt and glass/basalt fibres to facilitate the eco-efficiency analysis as stated above. The study aims to evaluate the environmental impacts associated with the production, use, and disposal of these hybrid composites. By comparing the LCA results of carbon/basalt and glass/basalt hybrid composites, the research seeks to identify the eco-efficient options and provide insights into their potential applications in various industries.

Specifically, the study will: (1) Quantify the environmental impacts of hybrid composites reinforced by carbon/basalt and glass/basalt fibres across their entire life cycle, including raw material extraction, manufacturing, usage, and end-of-life disposal; (2) Compare the sustainability performance of carbon/basalt and glass/basalt hybrid composites to determine which combination offers a lower environmental footprint; (3) Identify the key factors contributing to the environmental impacts of these hybrid composites and suggest potential improvements in their design and manufacturing processes; (4) Offer recommendations for the use of hybrid composites in various applications, based on their environmental performance and potential benefits.

By achieving these objectives, the study aims to contribute to the development of more sustainable composite materials and support the advancement of environmentally friendly technologies in the materials science and engineering fields.

2. Methodology

2.1. Materials

In this study, interlayer structured hybrid composites are considered. A hybrid composite specimen is 100 (L) × 10 (W) × 2 (T) mm^3, and contains 8 layers of equal thicknesses. An epoxy is chosen to be the matrix. For the carbon/basalt hybrid composite, each layer is reinforced by either high-strength carbon fibre or basalt fibre. For the glass/basalt hybrid composite, each layer is reinforced by either E glass fibre or basalt fibre. The properties of fibres and epoxy resin are shown in Table 1, based on the data from the literature [10,34–36]. It should be noted that due to the lack of direct and consistent information, the cost of basalt fibre is approximated to be ten times lower than that of carbon fibre.

Table 1. Constituent material properties [10,34–36].

Material	Elastic Modulus (GPa)	Tensile Strength (MPa)	Density (g/cm³)	Cost ($/L)
Epoxy	3.1	69.6	1.09	26.2
High strength carbon fibre	230	4900	1.8	151.2
E glass fibre	72	3450	2.58	10.8
Basalt fibre	89	2800	2.8	15.12

2.2. FEA-Based Model

Based on the design rules from a previous study, several possible layups are identified. For each layup, the fibre volume fractions can be adjusted to meet the required flexural strength. The composite layup is defined in Ansys ACP, and the three-point bend test in accordance with procedure A of ASTM D7264/D7264M-15 is simulated in Ansys Mechanical, following the same approach in a previous study [37].

The regression-based model is achieved using the equation shown below (Equation (1)). The formula is manipulated to make V_{fb} the dependent variable whilst V_{fc} is the independent variable, and the flexural strength value (S_F) is a pre-determined control variable. By manipulating V_{fc} between 30% and 70%, the corresponding value for V_{fb} is obtained. The constants, $c_0, c_1, c_2, c_3, c_4,$ and c_5, were calculated by using the Least Squares Estimation (LSE) method.

$$S_F = c_0 + c_1 V_{fc} + c_2 V_{fb} + c_3 V_{fc} + c_4 V_{fc}^2 + c_5 V_{fc}^2 \tag{1}$$

This process facilitates for examining, how different fibre volume fraction combination of each reinforcing fibres affects the flexural strength of each hybrid composite layup.

For the carbon/basalt fibre-reinforced hybrid composite, possible optimal layups are shown in Table 2. For each layup, left to right corresponds to ply 8 to ply 1, and C and B denote carbon/epoxy and basalt epoxy, respectively. For example, layup [B₂C₆] denotes plies 8-7 are basalt/epoxy and plies 6-1 are carbon/epoxy.

Table 2. Possible optimal layups for carbon/basalt fibre-reinforced hybrid composite.

Layup (Ply 8–Ply 1)	Number of Basalt/Epoxy Plies
[C₈]	0
[B₂C₆]	1
[B₃C₅]	3
[C₂B₂]ₛ	4
[CB₂C]ₛ	4
[(BC)₄]	4
[B₂C₂]ₛ	4
[B₂C₂B₃C]	5
[B₂CB₄C]	6
[CB₃]ₛ	6
[B₈]	8

For the glass/basalt fibre-reinforced hybrid composite, possible optimal layups are shown in Table 3. Similarly, for each layup, left to right corresponds to ply 8 to ply 1, and G and B denote glass/epoxy and basalt epoxy, respectively. For example, layup [G₇B] denotes plies 8-2 are glass/epoxy and ply 1 is basalt/epoxy.

Table 3. Possible optimal layups for glass/basalt fibre-reinforced hybrid composite.

Layup (Ply 8–Ply 1)	Number of Basalt/Epoxy Plies
[G₈]	0
[G₇B]	1
[(G₃B)₂]	2
[G₂BG₄B]	2
[BG₃]ₛ	2
[G₂B₂G₃B]	3
[G₃BG₂B₂]	3
[BG₅B₂]	3
[B₂G₅B]	3
[(G₂B₂)₂]	4
[GB₂G₃B₂]ₛ	4
[GB₃G₃B]	4

[G$_3$BGB$_3$]	4
[B$_2$G$_2$]$_S$	4
[G$_2$B$_2$GB$_3$]	5
[GB$_3$G$_2$B$_2$]	5
[B$_3$G$_3$B$_2$]	5
[G$_2$B$_6$]	6
[(G$_1$B$_3$)$_2$]	6
[B$_4$G$_2$B$_2$]	6
[B$_3$G]$_S$	6
[GB$_7$]	7
[B$_8$]	8

2.3. Determination of Candidates

For each of the layups in Tables 2 and 3, the effects of ply fibre volume fractions on the flexural strength are investigated by setting each of the ply volume fractions at three levels: 30%, 50%, and 70%. For a hybrid composite containing two types of fibres, there are 9 combinations. The flexural strengths for these 9 combinations are obtained using the developed FEA-based model. A regression-based model is then developed in the form of a polynomial containing two-ply fibre volume fractions, e.g., the fibre volume fraction of carbon/epoxy plies, V_{fc}, and the fibre volume fraction of basalt/epoxy plies, V_{fb}.

For the carbon/basalt fibre-reinforced hybrid composite, 2 levels of the minimum required flexural strength are considered, *i.e.*, 900 and 1300 MPa. For each minimum required flexural strength, several candidates are obtained using the regression-based models for the possible layups in Table 2. Similarly, for the glass/basalt fibre-reinforced hybrid composite, 2 levels of the minimum required flexural strength are considered, *i.e.*, 900 and 1200 MPa, and the candidates are obtained based on the layups in Table 3. The densities and costs of these derived candidates are calculated based on the constituent properties and compositions.

The classification is based on flexural strength because it is a critical parameter for assessing the mechanical performance of hybrid composites, particularly in structural applications where bending loads are prevalent. Flexural strength provides insights into the composite's ability to resist failure under bending, which is relevant for applications such as beams, panels, and other load-bearing components.

While elastic modulus is also an important property, it primarily reflects the stiffness of the material rather than its ultimate failure resistance. In hybrid composites, strength-related properties are often more sensitive to microstructural features such as fibre-matrix adhesion and defect distribution, making flexural strength a more suitable parameter for classification in this context.

2.4. Eco-Efficiency Assessment

The eco-efficiency (EE) performance of technically feasible 3D printed parts was assessed to determine whether parts could be manufactured with reduced environmental impact whilst not entailing excessive cost. Firstly, ELCA and LCC tools were used to determine the environmental impacts and life cycle costs of carbon/basalt and glass/basalt fibres composite layups. To perform these two analyses, LCI for each layup had to be developed by quantifying relevant inputs and outputs from the cradle to gate life cycle stages of the product. The inputs and outputs of the LCI were entered into the ELCA software (Simapro SimaPro, version 9.6.0.1) to determine the relevant life cycle environmental impacts (LCEI). The unit cost values of inputs in the LCI were used to estimate LCC.

The EE framework combines the LCC assessment with the ELCA to create an EE portfolio for each product. To integrate LCEI with LCC, these values were first normalised such that both parameters have common denominators, which ensures comparability and decreases complexity [38]. The EI values had to be normalised by dividing by the gross domestic environmental impact (GDEI/Inh) per inhabitant, whereas LCC values were normalised by dividing by the gross domestic product (GDP) per Australian inhabitant.

There are four stages in a life cycle assessment (LCA) with the objective to assess the economic and environmental feasibility of the carbon/basalt and glass/basalt fibre-reinforced hybrid composites. The four stages for LCA, in accordance with international standards ISO14040 44 (ISO 2006) [39], are scope and goal definition, inventory analysis, impact assessment, and interpretation of results. The objective of this study is to compare the economic and environmental efficiency of the optimal candidates for the carbon/basalt and glass/basalt fibre-reinforced hybrid composites and thus determine the sustainable ones.

The scope of this LCA follows a 'cradle to gate' approach accounting for all system inputs and outputs involved in the mining of required elements for material construction, transport of all materials to a composite manufacturing facility, and the manufacturing of the laminated hybrid composite, including energy used. The economic cost and environmental indicator (EI) of manufacturing 1 m^3 of composite material are considered throughout this analysis. The functional unit used for environmental and economic analysis is the cost and flexural strength (AUD/MPa) ratio. The unit used for transportation travels a ton of kilometres (tkm).

For the inventory analysis, a detailed list of all inputs and outputs for each stage of the life cycle must be obtained. This step is vital as the selected inputs and outputs will determine the EIs associated with hybrid composites. The inputs used for the inventory include details regarding composite density, manufacturing energy, ton kilometre travelled, and cost per litre. Location plays a key role when considering environmental costs, as the same item made in separate locations will have varied EI. The materials used for hybrid composite construction include carbon fibre, glass basalt fibre, and a high-strength epoxy resin, each sourced from separate manufacturers. Table 4 describes the material source and distance travelled to Curtin University, Bentley, where the hybrid composite was manufactured. Tables 5 and 6 give details of the inventory inputs used for flexural strengths of 900 MPa and 1200 MPa, respectively. For simplicity, the only economic input considered for LCC is the cost of the materials used for the manufacture of hybrid composites.

Table 4. Details for calculating the ton/km values.

Material	Source	Location	Distance Travelled Sea (nm)	Distance Travelled Road (km)
Basalt Fibre	Kamenny Vek	Dubna, Russia	9393	1784
Glass Fibre	Regina Glass	Victoria, Australia	1720	137
HS Epoxy	ATL Composites	Queensland, Australia	2662	98

Table 5. Life cycle inventory inputs for 900 MPa flexural strength.

	Materials					tkm		
Layup	Basalt Fibre	Glass Fibre	High Strength Epoxy	Kg/L	MJ	Sea	Road	Cost/L
[BG$_3$]$_s$	0.467	0.581	0.656	1.704	5.282	13.197	0.977	20.797
[(G$_2$B$_2$)$_2$]	0.410	0.768	0.600	1.778	5.511	12.526	0.896	19.917
[G$_3$BG$_2$B$_2$]	0.309	0.922	0.576	1.807	5.601	11.137	0.734	19.413
[G$_2$BG$_4$B]	0.234	1.064	0.546	1.844	5.717	10.143	0.617	18.876
[G$_2$BG$_4$B]	0.209	1.093	0.544	1.846	5.723	9.787	0.576	18.808
[G$_7$B]	0.177	1.129	0.542	1.848	5.727	9.338	0.524	18.727
[G$_7$B]	0.102	1.235	0.527	1.864	5.778	8.297	0.403	18.406
[BG$_3$]$_s$	0.203	1.304	0.457	1.964	6.089	9.928	0.585	17.573

Table 6. Life cycle inventory input data for 1200 MPa flexural strength.

	Materials				Mfg	tkm		
Layup	Basalt Fibre	Glass Fibre	High Strength Epoxy	(kg/L)	MJ	Sea	Road	Cost/L
[G$_3$BG$_2$B$_2$]	0.488	1.129	0.416	2.033	6.301	14.115	1.065	17.440
[BG$_3$]$_s$	0.472	1.161	0.409	2.042	6.331	13.918	1.042	17.310
[G$_2$BG$_4$B]	0.471	1.198	0.394	2.063	6.394	13.937	1.043	17.096
[G$_2$BG$_4$B]	0.317	1.355	0.390	2.061	6.390	11.743	0.790	16.799
[G$_7$B]	0.235	1.501	0.361	2.097	6.502	10.643	0.661	16.263
[G$_7$B]	0.181	1.580	0.349	2.111	6.543	9.898	0.574	16.016
[(G$_2$B$_2$)$_2$]	0.669	0.903	0.439	2.010	6.231	16.650	1.359	18.037

Tables 7 and 8 give details of the inventory inputs used for flexural strengths of 900 MPa and 1300 MPa, respectively.

Table 7. LCI of the optimal candidates in the 900 MPa flexural strength group.

Stacking Sequence	Cost ($/L)	Density (kg/L) Carbon (ρ_c)	Density (kg/L) Basalt (ρ_b)	Density (kg/L) Epoxy (ρ_e)	Density (kg/L) Total (ρ_T)	Manufacturing Energy Input (MJ)	Sea (tkm)	Road (tkm)
[B$_3$C$_5$]	48.109	0.338	0.386	0.735	1.459	42.457	7.185	0.077
[(BC)$_4$]	47.604	0.333	0.435	0.719	1.487	43.272	7.323	0.079
[B$_2$C$_2$B$_3$C]	38.151	0.203	0.534	0.760	1.496	43.526	7.366	0.079
[B$_2$CB$_4$C]	32.797	0.135	0.702	0.735	1.572	45.743	7.741	0.083
[B$_8$]	21.120	0.000	1.284	0.590	1.874	54.533	9.229	0.099

Table 8. LCI of the optimal candidates in the 1300 MPa flexural strength group.

| Stacking Sequence | Cost ($/L) | Density (kg/L) | | | | Manufacturing Energy Input (MJ) | Sea (tkm) | Road (tkm) |
		Carbon (ρ_c)	Basalt (ρ_b)	Epoxy (ρ_e)	Total (ρ_T)			
[C$_8$]	83.290	0.822	0.000	0.592	1.414	41.155	6.965	0.075
[B$_2$C$_6$]	52.700	0.405	0.411	0.685	1.501	43.667	7.390	0.080
[B$_2$C$_2$B$_3$C]	36.129	0.203	1.045	0.561	1.808	52.609	8.903	0.096
[B$_2$CB$_4$C]	30.561	0.135	1.267	0.515	1.917	55.787	9.441	0.102
[B$_8$]	19.123	0.000	1.788	0.394	2.182	63.500	10.746	0.116

Using SimaPro LCA software, the data given in the inventory is analysed using the given methods to develop the required EI category results for each considered layup. The methods used by the software can be thought of as the underlying system that performs multiple calculations using given emissions databases to gain EI results. For the results of this LCA to remain consistent with related research, the steps taken in this paper align both with international standards and the "Best Practice Guide for Life Cycle Impact Assessment (LCIA) in Australia" [40]. The international standards dictate the mandatory steps required for the LCA, while the best practice guide gives recommendations for the best underlying methods of analysis to be used during the LCIA for obtaining midpoint indicator results. Following the work of Renouf et al. [40], fourteen environmental impact categories have been selected for use in this assessment, all of which are relevant to Australian conditions and are listed in Table 9 along with the gross domestic EI, which has been calculated using Australian per capita information [5]. Localised methods such as the Australian Indicator Set 2.0 are preferable for obtaining LCIA data, but for some indicators, these data sets are not applicable for which an equivalent European or global method has been used, as shown in Table 9.

Table 9. Recommended methods weightings and normalisation factors [40].

Environmental Impact Category	Unit	Gross Domestic Environmental Impact	Method Used	Weighting
Global Warming Potential	kg CO$_2$ eq	28,690	Australian Indicator Set	20
Eutrophication	kg PO$_4^{3-}$ eq	19	Australian Indicator Set	2.9
Water Depletion	m^3 H$_2$O	930	Australian Indicator Set	6.2
Land Use and Ecological Diversity	Ha a	26	Australian Indicator Set	20
Photochemical Smog	kg NMVOC eq	75	Environmental Footprints 3.1	2.8
Human Toxicity	1,4-DB eq	3216	ReciPe	2.7
Terrestrial Ecotoxicity	1,4-DB eq	88	ReciPe	10.3
Freshwater Ecotoxicity	1,4-DB eq	172	ReciPe	6.9
Marine Ecotoxicity	1,4-DB eq	12,117,106	Environmental Footprints 3.1	7.7
Ionising Radiation	kBq U-235 eq	1306	CML	1.9
Ozone Depletion	CFC-11 eq	0.002	CML	3.9
Abiotic Depletion	kg Sb eq	300	CML	8.2
Acidification	kg SO$_2$ eq	123	CML	3.1
Raspatory Inorganics	kg PM$_{2.5}$ eq	45	ReciPe	3.4

2.5. Eco-Efficicney Portfolio Analysis Methodology

Once the environmental impacts for all 900 MPa and 1200 MPa flexural strengths and the associated life cycle cost (LCC) for each layup have been determined, they are each normalised against the relevant gross domestic environmental impact (GDEI) and gross domestic income (GDP) for Australian conditions. Equation (2), which is used to gain the normalised value (NV_i) is used for normalising the life cycle environmental impact (LCEI) with the GDEI given in Table 9.

$$NV_{ei} = \frac{LCEI_{ei}}{GDEI_{ei}} \ (inh) \tag{2}$$

where '*ei*' refers to a specific environmental impact being considered and '*inh*' refers to the net capita of inhabitants.

Once normalised, the values are summed into a single value for normalised environmental impact (EI_n) by multiplying each impact value with an associated weight (W_{ei}) and summing the weighted values as demonstrated in Equation (3).

$$EI_n = \sum_{i=1}^{14} NV_{ei} \times W_{ei} \ (inh) \tag{3}$$

A normalised cost (NC_n) for each layup (n) can be obtained with a similar method where the GDP per capita in Australia is used as the normalising factor as can be seen in Equation (4).

$$NC_n = \frac{LCC_n}{GDP} \ (inh) \tag{4}$$

Using the normalised values for EI and life cycle cost obtained using Equations (3) and (4), the initial portfolio position for each layup, *n*, being considered can be obtained using Equation (5) for the initial environmental portfolio position (PP_{en}), and Equation (6) for the initial costing portfolio position (PP_{cn}).

$$PP_{en} = \frac{EI_n}{EI_{avg}} \tag{5}$$

$$PP_{cn} = \frac{NC_n}{NC_{avg}} \tag{6}$$

The values of EI_n and NC_n form the foundation on which the eco-efficiency portfolio analysis is constructed. To ensure that both EI and cost contribute equally to the analysis, an environmental impact to cost relevance factor (R) is used to adjust the initial portfolio positions. This relevance factor gives detail as to which is the dominant input between EI and cost.

$$R = \frac{EI_{avg}}{NC_{avg}} \tag{7}$$

Using the value obtained in Equation (7) for environmental impact to cost relevance, the final portfolio position for EI (PP'_{en}) and life cycle cost (PP'_{cn}) is obtained using Equations (8) and (9).

$$PP'_{en} = \frac{PP_{e,avg} + (PP_{en} - PP_{e,avg})(\sqrt{R})}{PP_{e,avg}} \tag{8}$$

$$PP'_{cn} = \frac{PP_{c,avg} + (PP_{cn} - PP_{c,avg})/(\sqrt{R})}{PP_{c,avg}} \tag{9}$$

The final portfolio positions can give a graphic representation of the values found for EI and the life cycle cost for each layup being considered. The normalised life cycle cost is plotted on the abscissa and the normalised EI is plotted on the ordinate. Note that the axis number line is in reverse; therefore, the point with the least EI and the least life cycle cost would be found in the top right corner of the figure, indicating high eco-efficiency, while the highest scoring point in both categories would be found in the bottom left corner, indicating low eco-efficiency. The diagonal line represents the border between high and low eco-efficiency. The subsequent eco-efficiency portfolio is ideal for comparing multiple hybrid composite layup options, which is a key goal of this research.

3. Results and Discussion

3.1. Candidates

The candidates for the carbon/basalt fibre-reinforced hybrid composite with the minimum required flexural strengths 900 MPa and 1300 MPa are given in Tables 10 and 11, respectively.

Table 10. Candidates for the carbon/basalt fibre-reinforced hybrid composite with the minimum required flexural strength 900 MPa.

Layup	V_{fc}	V_{fb}	Density (g/cm^3)	Cost ($/L)
[B$_3$C$_5$]	0.390	0.300	1.456	55.421
[B$_3$C$_5$]	0.350	0.331	1.458	52.168
[B$_3$C$_5$]	0.300	0.368	1.459	48.109
[(BC)$_4$]	0.370	0.311	1.487	47.604
[B$_2$C$_2$B$_3$C]	0.300	0.305	1.496	38.151
[B$_2$CB$_4$C]	0.330	0.300	1.533	34.018
[B$_2$CB$_4$C]	0.300	0.334	1.572	32.797
[B$_8$]	0.000	0.458	1.874	21.120

Table 11. Candidates for the carbon/basalt fibre-reinforced hybrid composite with the minimum required flexural strength 1300 MPa.

Layup	V_{fc}	V_{fb}	Density (g/cm^3)	Cost ($/L)
[C$_8$]	0.457	0.000	1.414	83.290
[B$_2$C$_6$]	0.300	0.587	1.501	52.700
[B$_2$C$_2$B$_3$C]	0.580	0.306	1.571	51.269
[B$_2$CB$_4$C]	0.660	0.307	1.601	44.274
[B$_2$CB$_4$C]	0.650	0.317	1.612	43.877
[B$_2$CB$_4$C]	0.600	0.366	1.665	41.912
[B$_2$CB$_4$C]	0.550	0.411	1.714	39.976
[B$_2$CB$_4$C]	0.500	0.453	1.759	38.062
[B$_2$CB$_4$C]	0.450	0.493	1.802	36.167
[B$_2$C$_2$B$_3$C]	0.300	0.597	1.808	36.129
[B$_2$CB$_4$C]	0.400	0.531	1.842	34.286
[B$_2$CB$_4$C]	0.350	0.568	1.880	32.418
[B$_2$CB$_4$C]	0.300	0.603	1.917	30.561
[B$_8$]	0.000	0.639	2.182	19.123

The candidates for the glass/basalt fibre-reinforced hybrid composite with the minimum required flexural strengths 900 MPa and 1200 MPa are given in Tables 12 and 13, respectively.

Table 12. Candidates for the glass/basalt fibre-reinforced hybrid composite with the minimum required flexural strength 900 MPa.

Layup	V_{fg}	V_{fb}	Density (g/cm^3)	Cost ($/L)
[BG$_3$]$_S$	0.692	0.300	1.704	20.797
[G$_2$B$_2$GB$_3$]	0.305	0.595	1.730	20.627
[BG$_3$]$_S$	0.650	0.350	1.743	20.339
[G$_3$BGB$_3$]	0.306	0.580	1.769	20.020
[(G$_2$B$_2$)$_2$]	0.304	0.595	1.778	19.917
[BG$_3$]$_S$	0.605	0.400	1.781	19.885
[G$_3$BGB$_3$]	0.377	0.550	1.803	19.853
[G$_2$B$_2$]$_2$	0.379	0.550	1.805	19.842
[G$_3$BG$_2$B$_2$]	0.305	0.572	1.807	19.413
[G$_3$BG$_2$B$_2$]	0.362	0.550	1.821	19.387
[(G$_3$B)$_2$]	0.305	0.551	1.829	18.982
[(G$_3$B)$_2$]	0.309	0.550	1.829	18.983
[G$_2$BG$_4$B]	0.347	0.550	1.844	18.876
[G$_2$BG$_4$B]	0.322	0.560	1.845	18.830
[G$_2$BG$_4$B]	0.310	0.565	1.846	18.808
[G$_7$B]	0.525	0.500	1.848	18.727
[G$_7$B]	0.302	0.547	1.864	18.406
[BG$_3$]$_S$	0.398	0.600	1.921	18.155
[BG$_3$]$_S$	0.334	0.650	1.951	17.756
[BG$_3$]$_S$	0.301	0.674	1.964	17.573

Table 13. Candidates for the glass/basalt fibre-reinforced hybrid composite with the minimum required flexural strength 1200 MPa.

Layup	V_{fg}	V_{fb}	Density (g/cm^3)	Cost ($/L)
[B$_2$G$_2$]$_S$	0.618	0.400	1.886	19.657
[BG$_5$B$_2$]	0.700	0.430	1.913	19.122
[BG$_5$B$_2$]	0.692	0.450	1.927	18.961
[B$_2$G$_5$B]	0.701	0.465	1.946	18.779
[BG$_5$B$_2$]	0.673	0.500	1.962	18.560
[B$_2$G$_5$B]	0.688	0.500	1.971	18.499
[BG$_5$B$_2$]	0.654	0.550	1.997	18.159
[B$_2$G$_5$B]	0.668	0.550	2.005	18.101
[G$_2$B$_2$]$_2$	0.495	0.700	2.010	18.037
[G$_3$BGB$_3$]	0.497	0.700	2.011	18.029
[GB$_3$G$_3$B]	0.516	0.700	2.027	17.922
[BG$_5$B$_2$]	0.635	0.600	2.032	17.758
[G$_2$B$_2$G$_3$B]	0.477	0.700	2.030	17.457
[G$_3$BG$_2$B$_2$]	0.482	0.700	2.033	17.440
[BG$_3$]$_S$	0.700	0.600	2.042	17.310
[G$_2$BG$_4$B]	0.698	0.619	2.063	17.096
[G$_2$BG$_4$B]	0.668	0.630	2.063	17.054
[G$_2$BG$_4$B]	0.612	0.650	2.063	16.979
[G$_2$BG$_4$B]	0.470	0.700	2.061	16.799
[G$_3$B]$_2$	0.533	0.700	2.087	16.622
[G$_7$B]	0.697	0.665	2.097	16.263
[G$_7$B]	0.537	0.700	2.111	16.016

These candidates form so-called Pareto fronts, as shown in Figure 1. It is shown the density and cost are inversely related, and the glass/basalt fibre-reinforced hybrid composite has significantly smaller ranges for the cost and density compared to the carbon/basalt one.
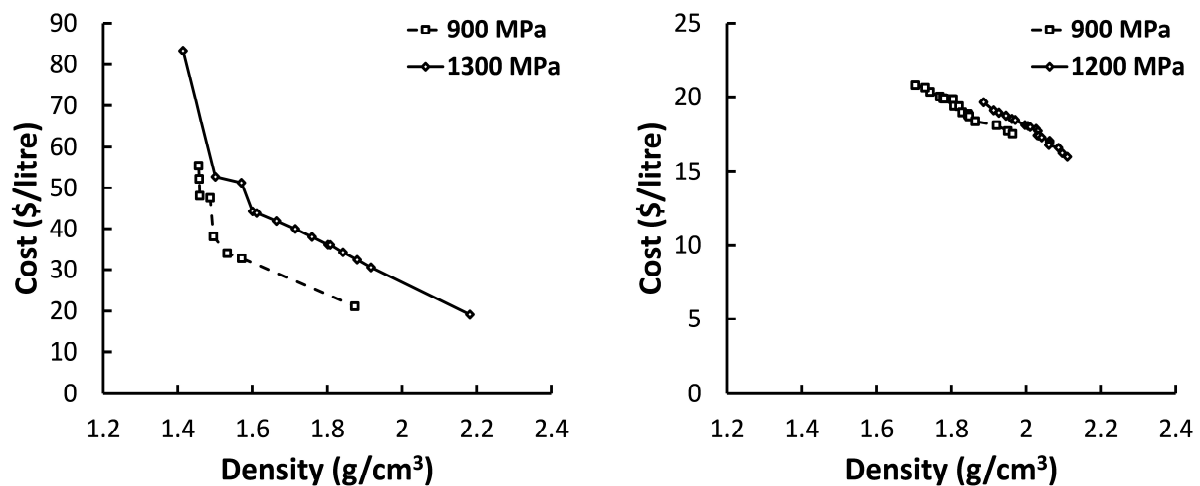
Figure 1. Pareto fronts for the carbon/basalt (**left**) and glass/basalt (**right**) fibre-reinforced hybrid composites.

3.2. Eco-Efficiency Performance of Glass Basalt Hybrid Composites

Prime candidate layup options for flexural strength 900 MPa and 1200 MPa have been selected for further analysis by means of LCA, where the LCIA environmental indicators have been used, along with the economic cost, to develop an eco-efficiency portfolio. The costs and EIs will be calculated for the manufacture of one cubic metre of composite material. For comparison, the chosen candidates for basalt and glass fibre-reinforced hybrid composite are displayed in Table 14. For ease of comparison, each candidate layup has been given a code to be used throughout the analysis.

Table 14. Optimal layup designs for basalt and glass fibre-reinforced hybrid composites with a minimum flexural strength of 900 MPa and 1200 MPa.

900 MPa		1200 MPa	
Layup	Code	Layup	Code
$[BG_3]_S$	A	$[BG_3]_S$	A′
$[G_2B_2]_2$	B	$[G_2B_2]_2$	B′
$[G_3BG_2B_2]$	C	$[G_3BG_2B_2]$	C′
$[G_2BG_4B]$ more glass	D	$[G_2BG_4B]$ more glass	D′
$[G_2BG_4B]$	E	$[G_2BG_4B]$	E′
$[G_7B]$	F	$[G_7B]$	F′
$[G_7B]$ more glass	G	$[G_7B]$ more glass	G′

For each layup option, fourteen EI indicators were investigated, and the results can be used to identify the environmental 'hot spot' or indicator that has the greatest impact. Figures 2 and 3 have been developed using the normalised and weighted environmental indicators also known as eco points. For both 900 MPa and 1200 MPa, terrestrial ecotoxicity is the dominant EI or 'hotspot', followed by GWP. The terrestrial ecotoxicity could mainly have resulted from the use of epoxy in the hybrid composites (Figure 2). This epoxy resin is toxic to aquatic organisms, resulting in long-term adverse effects in the marine environment [41]. The content of epoxy decreases gradually from layups A to H, so layup A produces the highest overall impact (Table 2). The second largest impact of climate change is mainly from the manufacturing of glass. The glass industry contributes significantly to CO_2 emissions due to high temperature (1500 °C) production processes and the use of hydrocarbon-based fuels in the manufacturing process [42]. In the case of layups for 1200 MPa, a similar trend appeared to happen (Figure 3), but the glass contribution here is more than the ones for 900 MPa, because the content of glass in the former case was increased to increase the strength from 900 MPa to 1200 MPa. Whilst global warming impact is the second dominant impact, the overall impact has been decreased with the reduction of the terrestrial ecotoxicity impact.
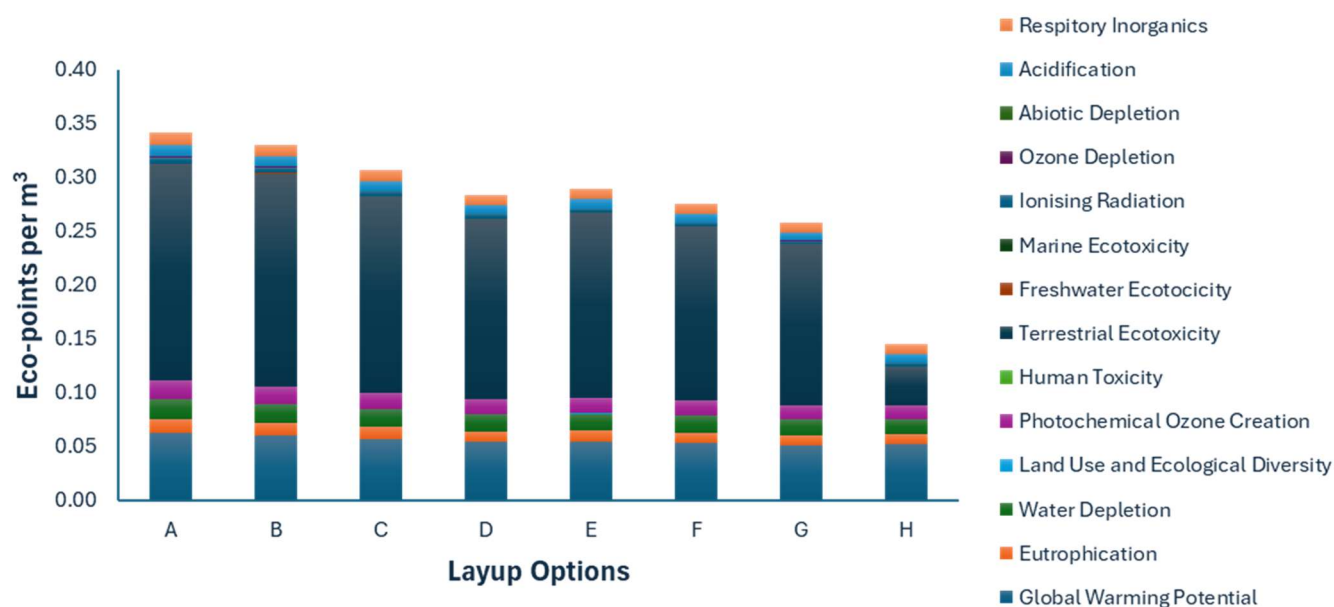
Figure 2. Environmental impacts in Ecopoints per m³ for glass basalt composites for 900 MPa flexural strength.
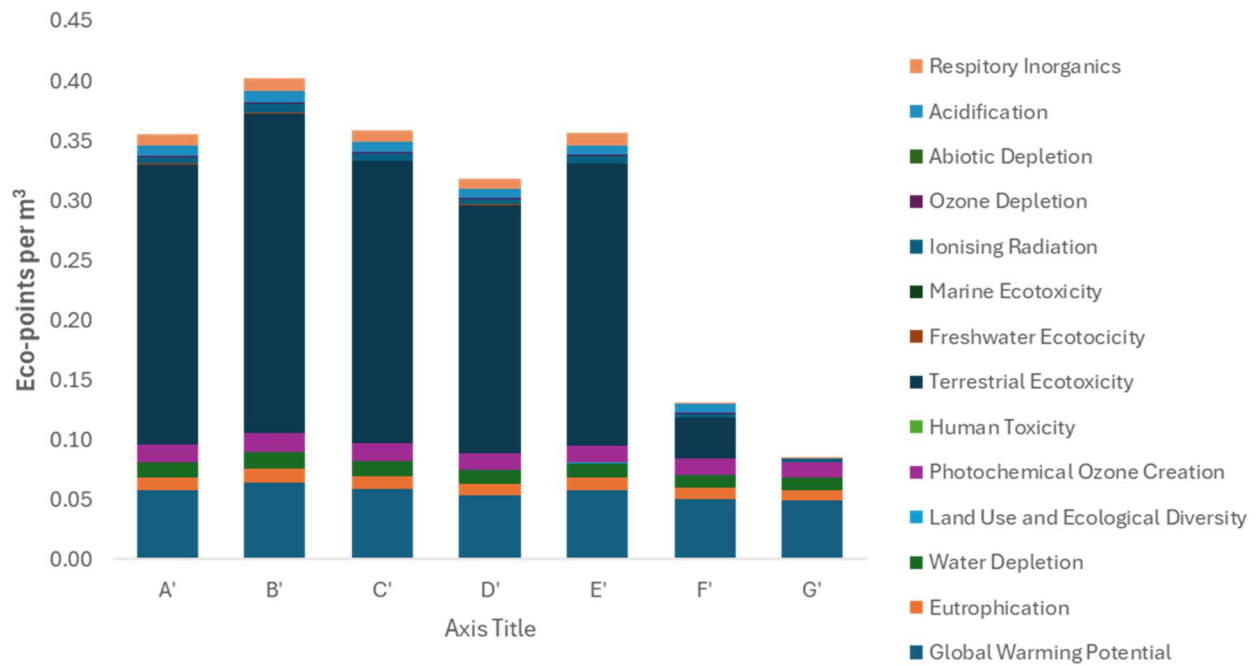
Figure 3. Environmental impacts in Ecopoints per m³ for glass basalt composites for 1200 MPa flexural strength.

The final portfolio position for economic cost and environmental impact of each optimal candidate is detailed in Figures 4 and 5. Note that only candidate designs that are above the diagonal line depicted in the graph should be considered for manufacture as they show high eco-efficiency. The layups using an increased amount of epoxy have not been found to be eco-efficient (Figure 4). The use of an increased amount of epoxy not only increased the environmental impacts but also the costs of the composites. The unit costs of epoxy ($30/kg) are around 10 times higher than the glass. Therefore, the composites A, B, C, E, F, A′, B′, C′, and D′ have not been found eco-efficient.
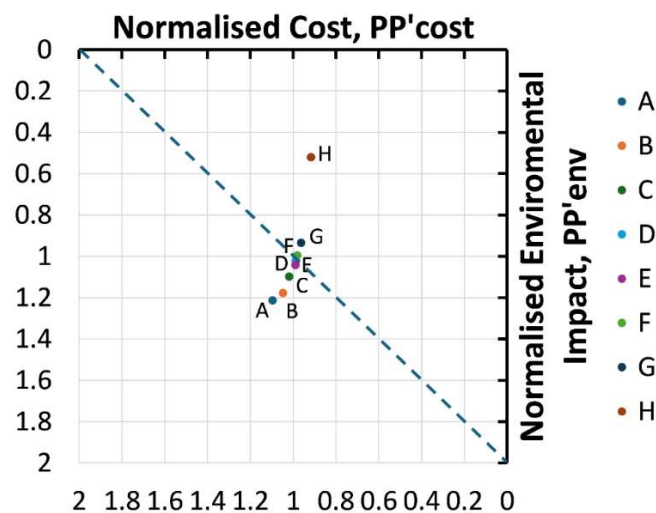
Figure 4. Eco-efficiency portfolio for 900 MPa flexural strength.

Of all the optimal candidates for flexural strength of 900 MPa, option H ([BG$_3$]$_S$, more glass) is seen to have the lowest normalised cost and the normalised lowest EI, thus the highest eco-efficiency. Other eco-efficient options include G ([G$_7$B], more glass) and F ([G$_7$B]), as they are both found above the diagonal line.

For flexural strength of 1200 MPa, option G′ ([G$_7$B], more glass) has the lowest normalised cost and lowest normalised EI, thus having the highest eco-efficiency. Design F′ ([G$_7$B]) is the only other optimal design that can be considered eco-efficient.
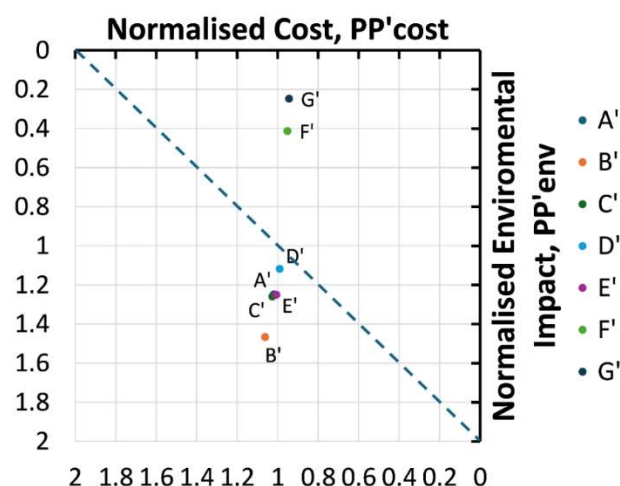
Figure 5. Eco-efficiency portfolio for 1200 MPa flexural strength.

3.3. Eco-Efficiency of Carbon Basalt Hybrid Composites

For comparison, the chosen candidates for basalt and glass fibre-reinforced hybrid composite are displayed in Table 15.

Table 15. Optimal layup designs for carbon and glass fibre-reinforced hybrid composites with a minimum flexural strength of 900 MPa and 1300 MPa.

900 MPa		1300 MPa	
Layup	Code	Layup	Code
$[B_3C_5]$	C	$[C_8]$	A′
$[(BC)_4]$	D	$[B_2C_6]$	B′
$[B_2C_2B_3C]$	E	$[B_2C_2B_3C]$	E′
$[B_2CB_4C]$	F	$[B_2C_2B_4C]$	F′
$[B_8]$	G	$[B_8]$	G′

Similar testing of the flexural strength of carbon/basalt fibre-reinforced hybrid composites has been conducted by Sun et al. [14]. The case study compared the experimentally obtained flexural strength of carbon/basalt fibre-reinforced hybrid composites with the flexural strength values obtained through FEA simulations as well as the analytically obtained values.

The flexural strength values obtained through FEA simulations followed a similar trend to those obtained through experimental testing [14]. The FEA values were consistently higher, which could be attributed to the parameter used in the simulations, but nonetheless, this case study testifies to the ability of FEA simulations to obtain flexural strengths of carbon/basalt fibre-reinforced hybrid composites.

Unlike glass basalt hybrid composites, carbon fibre use contributes to the overall impact as carbon fibre is very carbon intensive (*i.e.*, 25 kg CO_2eq/kg) [43]. This has increased the global warming impact, which in fact, increased the overall impact. Thus, the layups with the reduced levels of carbon contents have lower environmental impacts (Figures 6 and 7).
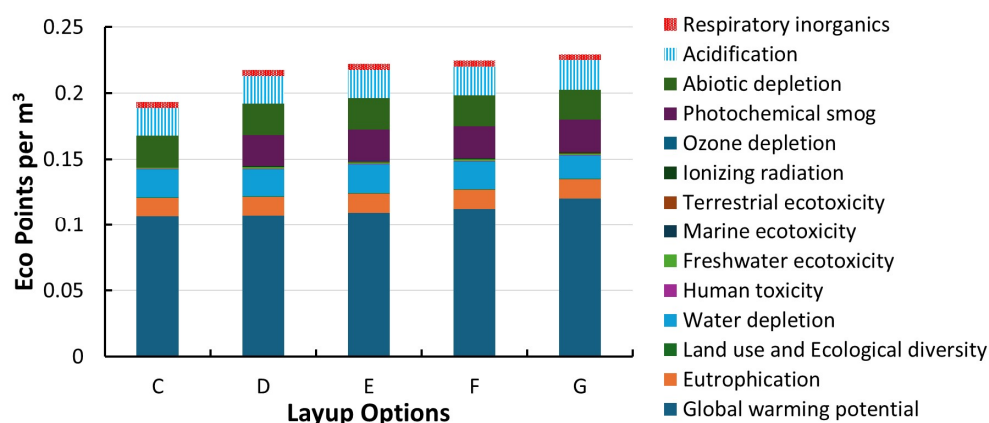

Figure 6. Environmental impacts in Ecopoints per m^3 for carbon basalt composites for 900 MPa flexural strength.
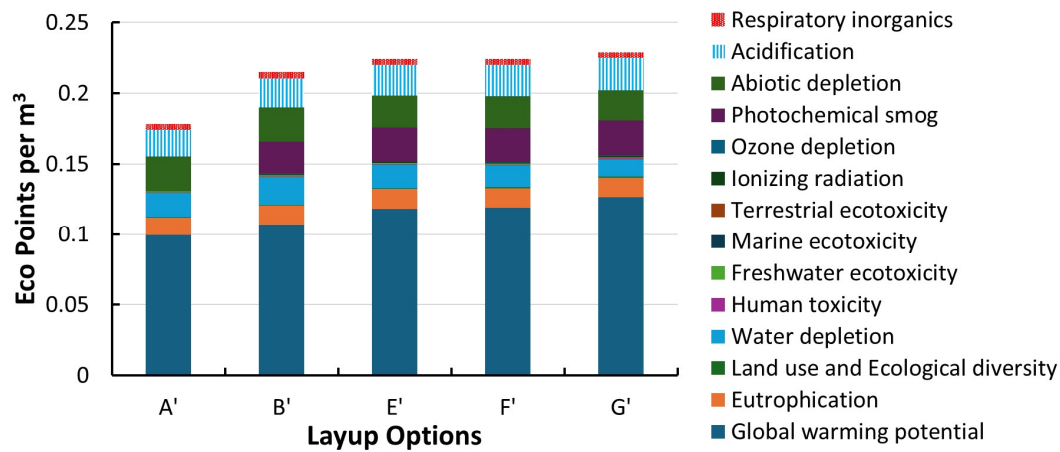
Figure 7. Environmental impacts in Ecopoints per m^3 for carbon basalt composites for 1300 MPa flexural strength.

For the 1300 MPa group, the stacking sequence [B$_8$] was also the most eco-efficient out of the group. Similar to the 900 MPa group, the cost to manufacture is the overwhelming factor that distinguishes the eco-efficiency of the optimal candidates (Figure 8). Since both [B$_8$] and [C$_8$] stacking sequences are both present in this group, a comprehensive comparison and observation can be made. First of all, the manufacturing cost difference between the two is the largest difference between any optimal candidates in any group. The [B$_8$] stacking sequence is 20% of the cost of the [C$_8$] stacking sequence. In other words, the cost to manufacture one cubic meter of [B$_8$] composite is five times cheaper than the same volume of composite made from [C$_8$]. In addition, as discussed in the previous section, the use of glass increased the overall environmental impacts.
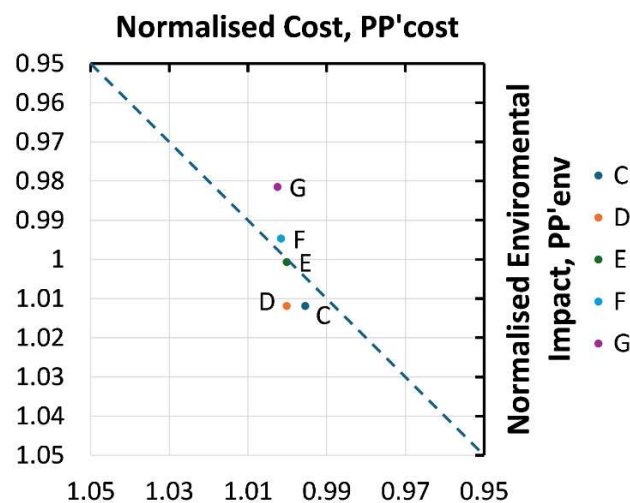

Figure 8. Eco-efficiency framework for the 900 MPa flexural strength group.

For the 1300 MPa group, the stacking sequence [B$_8$] was also the most eco-efficient out of the group. Similar to the 900 MPa group, the cost to manufacture is the overwhelming factor that distinguishes the eco-efficiency of the optimal candidates (Figure 9). Since both [B$_8$] and [C$_8$] stacking sequences are both present in this group, a comprehensive comparison and observation can be made. First of all, the manufacturing cost difference between the two is the largest difference between any optimal candidates in any group. The [B$_8$] stacking sequence is 20% the cost of the [C$_8$] stacking sequence. In other words, the cost to manufacture one cubic meter of [B$_8$] composite is five times cheaper than the same volume of composite made from [C$_8$].
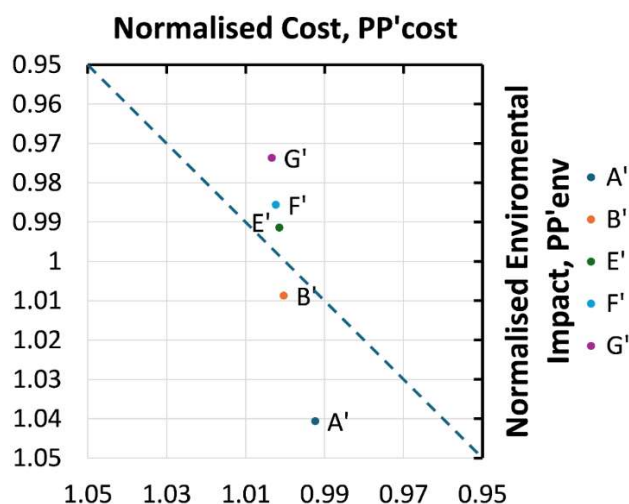
Figure 9. Eco-efficiency framework for the 1300 MPa flexural strength group.

Another similarity of the results thus far is that the higher basalt hybrid ratio candidates score a higher environmental impact value. In this case, approximately 28% higher environmental impact value.

4. Uncertainty Analysis

There could be uncertainties associated with the quality of the modelling-based inputs. The reliability of the results was determined by performing a Monte Carlo Simulation (MCS) uncertainty analysis. This simulation was conducted for this analysis by running 1000 iterations at a confidence interval of 95% to quantify the level of uncertainty in the inventory inputs (*i.e.*, materials energy and transportation) for stages of the hybrid composite material life cycle.

The MCS has been conducted on one of the hybrid composite materials (*i.e.*, F′ or G_7B using glass fibre) (Table 16) to see the level of uncertainty with the values of the calculated impacts. The calculated coefficient of variation (CV) of the abiotic depletion, global warming potential, acidification, respiratory organics, eutrophication, photochemical smog, and water use at less than 10% infers that the degree of uncertainty in the calculated impact is relatively small based on [44,45]. These environmental impacts have acceptable CV due to the fact that the impacts are not directly affected by the variation in topography, water bodies, vegetation coverage, and land use changes. However, discrepancies were found in more regional and local impact categories (*i.e.*, land use and ecotoxicities) due to the aforementioned reasons [46].

Table 16. Uncertainty analysis of environmental impact results of G_7B hybrid composite using Monte Carlo simulation.

Impact Category	Unit	Mean	Median	CV (%)
Abiotic depletion	kg Sb eq	5.35×10^{-7}	5.34×10^{-7}	0.6
acidification	kg SO_2 eq	0.02	0.02	3
Ozone layer depletion (ODP)	kg CFC-11 eq	1.09×10^{-9}	1.024×10^{-9}	32
Human carcinogenic toxicity	kg 1,4-DCB	0.0011	0.0011	16
Human non-carcinogenic toxicity	kg 1,4-DCB	6.00×10^{-4}	5.87×10^{-4}	11
Marine ecotoxicity	kg 1,4-DCB	1.60×10^{-4}	1.12×10^{-4}	104
Terrestrial ecotoxicity	kg 1,4-DCB	4.40×10^{-3}	0.0042	35
Eutrophication	kg PO_4 eq	4.41×10^{-3}	4.37×10^{-3}	7
Global Warming	kg CO_2	5.4	5.39	3
Land use	Ha a	1.25×10^{-5}	1.20×10^{-5}	27
Water Use	M3 H_2O	0.15	0.15	0.43
Ionising radiation	kBq U-235 eq	0.004	0.003	57
Photochemical ozone formation	kg NMVOC eq	0.03	0.03	7
Respiratory organics	kg $PM_{2.5}$ eq	0.04	0.04	6

5. Conclusions

In this study, an FEA-based modelling approach was used to simulate the flexural behaviour of carbon/basalt and glass/basalt fibre-reinforced hybrid composites. The results show that increasing the fibre volume fraction generally enhances flexural strength by improving load transfer between the fibres and the matrix.

The optimal design candidates for each given flexural strength were chosen from the Pareto front of design points. A cost density score was used to select the optimal option in each case. For a given flexural strength of 900 MPa, layup option [G_7B] is the optimal candidate, while [$(G_3B)_2$] is an acceptable choice. For a given flexural strength of 1200 MPa, layup option [BG_5B_2] is the optimal choice, while layup [G_2BG_4B] is second best. The optimised designs for 900 MPa and 1200 MPa were selected for further analysis through a life cycle assessment and eco-efficiency assessment. The environmental impact analysis using SimpaPro software identified the environmental impacts for all candidate designs considered. Terrestrial ecotoxicity has been found to be a hotspot for the designs of both 900 MPa and 1200 MPa flexural strengths, contributing over 50% of eco-points across all designs. GWP should also be considered a threat for all designs considered. Economic and environmental analysis of the manufacturing process, through eco-efficiency portfolio analysis, separates eco-efficient designs from those that are sub-optimal. The designs with the highest eco-efficiency for 900 MPa and 1200 MPa flexural strength are [BG_3]s, more glass, and [G_7B], more glass, respectively. Epoxy is noted to be the main concern both economically and environmentally, as it is costly and hard to recycle. All designs that used relatively less epoxy were considered eco-efficient.

In the case of carbon/basalt fibre-reinforced hybrid composite, it was concluded in the life cycle assessment portion of the study that even though the production process of basalt fibres is considerably less environmentally harmful compared to the production process of carbon fibres, the extra basalt fibre needed to achieve the minimum flexural strengths has offset the difference. This has caused the stacking sequence that utilises more basalt fibres to be more environmentally harmful in the end. However, due to the wide discrepancy between the cost of basalt and carbon fibres, the stacking sequences that utilises more basalt fibres on average were 30% cheaper than a carbon fibre-rich stacking sequence.

A possible design criterion for carbon/basalt fibre-reinforced hybrid composite is the [B_2CB_4C] stacking sequence, which was the most versatile stacking sequence of the lot. An optimal candidate for all minimum flexural strength requirements, and nearly half of all the identified optimal candidates, was a variance of [B_2CB_4C] stacking sequences. [B_2CB_4C] was the second most eco-efficient in both 900 and 1300 MPa flexural strength groups. Lastly, the 51:20 economic gain to environmental loss ratio states that the increase in the environmental impact that carbon/basalt fibre-reinforced hybrid composite poses can be justified due to the exponential economic gain that basalt fibres can offer.

In real applications of composite materials, design variables are not always deterministic due to manufacturing tolerances and the presence of defects such as matrix voids, resin-rich regions, and variations in fibre-matrix adhesion [47]. These factors can influence the mechanical performance of composites and introduce uncertainties in real-world applications. While this study assumes ideal manufacturing conditions to focus on the fundamental relationships between design parameters and material performance, future work could explore the impact of these manufacturing challenges. Nevertheless, the conclusions drawn here provide valuable insights that remain applicable to real-world applications, particularly for guiding initial design decisions and optimization strategies.

Author Contributions

Conceptualization, G.H., R.C., W.B. and C.D.; Methodology, G.H, R.C., W.B. and C.D.; Software, G.H., R.C., W.B. and C.D.; Validation, G.H. and R.C.; Formal Analysis, G.H. and R.C.; Investigation, G.H. and R.C.; Resources, G.H. and R.C.; Data Curation, G.H. and R.C.; Writing—Original Draft Preparation, G.H. and R.C.; Writing—Review & Editing, W.B. and C.D.; Visualization, G.H. and R.C.; Supervision, W.B. and C.D.; Project Administration, W.B.

Ethics Statement

Not Applicable.

Informed Consent Statement

Not Applicable.

Data Availability Statement

The authors confirm that the data supporting the findings of this study are available within the paper.

Funding

Declaration of Competing Interest

The authors declare that they have no known competing financial interests or personal relationships that could have appeared to influence the work reported in this paper.

References

1. Sharma H, Kumar A, Rana S, Sahoo NG, Jamil M, Kumar R, et al. Critical review on advancements on the fiber-reinforced composites: Role of fiber/matrix modification on the performance of the fibrous composites. *J. Mater. Res. Technol.* **2023**, *26*, 2975–3002. doi:10.1016/j.jmrt.2023.08.036.
2. Khalid MY, Al Rashid A, Arif ZU, Ahmed W, Arshad H, Zaidi AA. Natural fiber reinforced composites: Sustainable materials for emerging applications. *Results Eng.* **2021**, *11*, 100263. doi:10.1016/j.rineng.2021.100263.
3. Ravishankar B, Nayak S, Kader M. Hybrid composites for automotive applications—A review. *J. Reinf. Plast. Compos.* **2019**, *38*, 073168441984970. doi:10.1177/0731684419849708.
4. Qureshi J. A Review of Fibre Reinforced Polymer Structures. *Fibers* **2022**, *10*, 27.
5. Biswas W, Dong C. Eco-Efficiency Performance for Multi-Objective Optimal Design of Carbon/Glass/Flax Fibre-Reinforced Hybrid Composites. *Sustainability* **2024**, *16*, 2928.
6. Sienkiewicz N, Dominic M, Parameswaranpillai J. Natural Fillers as Potential Modifying Agents for Epoxy Composition: A Review. *Polymers* **2022**, *14*, 265.
7. Sapuan SM, Aulia HS, Ilyas RA, Atiqah A, Dele-Afolabi TT, Nurazzi MN, et al. Mechanical Properties of Longitudinal Basalt/Woven-Glass-Fiber-reinforced Unsaturated Polyester-Resin Hybrid Composites. *Polymers* **2020**, *12*, 2211.
8. Patti A, Nele L, Zarrelli M, Graziosi L, Acierno D. A Comparative Analysis on the Processing Aspects of Basalt and Glass Fibers Reinforced Composites. *Fibers Polym.* **2021**, *22*, 1449–1459. doi:10.1007/s12221-021-0184-x.
9. Abdulrahman J, Ebhota WS, Tabakov PY. Biopolymer Composite Materials in Oil and Gas Sector. *Int. J. Polym. Sci.* **2024**, *2024*, 8584879. doi:10.1155/2024/8584879.
10. Chowdhury IR, Pemberton R, Summerscales J. Developments and Industrial Applications of Basalt Fibre Reinforced Composite Materials. *J. Compos. Sci.* **2022**, *6*, 367.
11. Protchenko K, Zayoud F, Urbański M, Szmigiera E. Tensile and Shear Testing of Basalt Fiber Reinforced Polymer (BFRP) and Hybrid Basalt/Carbon Fiber Reinforced Polymer (HFRP) Bars. *Materials* **2020**, *13*, 5839.
12. Militký J, Kovačič V, Křemenáková D, Šesták J, Holeček M, Málek J. Basalt filaments—properties and applications. In *Some Thermodynamic, Structural and Behavioral Properties of Materials Accentuating Noncrystalline States*; OPS-ZČU: Plzeň, Czech Republic, 2005; pp. 499–520.
13. Chen X, Zhang Y, Hui D, Chen M, Wu Z. Study of melting properties of basalt based on their mineral components. *Compos. Part B Eng.* **2017**, *116*, 53–60. doi:10.1016/j.compositesb.2017.02.014.
14. Sun G, Tong S, Chen D, Gong Z, Li Q. Mechanical properties of hybrid composites reinforced by carbon and basalt fibers. *Int. J. Mech. Sci.* **2018**, *148*, 636–651. doi:10.1016/j.ijmecsci.2018.08.007.
15. Fiore V, Scalici T, Di Bella G, Valenza A. A review on basalt fibre and its composites. *Compos. Part B Eng.* **2015**, *74*, 74–94. doi:10.1016/j.compositesb.2014.12.034.
16. Agrawal M, Gupta M, Durai Prabhakaran RT, Mahajan P. A comparative study of static and fatigue performance of glass and basalt fiber reinforced epoxy composites. *Polym. Compos.* **2024**, *45*, 3551–3565. doi:10.1002/pc.28008.
17. Patti A, Acierno S, Nele L, Graziosi L, Acierno D. Sustainable Basalt Fibers vs. Traditional Glass Fibers: Comparative Study on Thermal Properties and Flow Behavior of Polyamide 66-Based Composites. *ChemEngineering* **2022**, *6*, 86.
18. Ary Subagia IDG, Kim Y, Tijing LD, Kim CS, Shon HK. Effect of stacking sequence on the flexural properties of hybrid composites reinforced with carbon and basalt fibers. *Compos. Part B Eng.* **2014**, *58*, 251–258. doi:10.1016/j.compositesb.2013.10.027.
19. Fiore V, Di Bella G, Valenza A. Glass–basalt/epoxy hybrid composites for marine applications. *Mater. Des.* **2011**, *32*, 2091–2099. doi:10.1016/j.matdes.2010.11.043.
20. Bozkurt ÖY. Hybridization effects on tensile and bending behavior of aramid/basalt fiber reinforced epoxy composites. *Polym. Compos.* **2017**, *38*, 1144–1150. doi:10.1002/pc.23677.
21. Sarasini F, Tirillò J, Valente M, Valente T, Cioffi S, Iannace S, et al. Effect of basalt fiber hybridization on the impact behavior under low impact velocity of glass/basalt woven fabric/epoxy resin composites. *Compos. Part A Appl. Sci. Manuf.* **2013**, *47*, 109–123. doi:10.1016/j.compositesa.2012.11.021.
22. Sarasini F, Tirillò J, Valente M, Ferrante L, Cioffi S, Iannace S, et al. Hybrid composites based on aramid and basalt woven fabrics: Impact damage modes and residual flexural properties. *Mater. Des.* **2013**, *49*, 290–302. doi:10.1016/j.matdes.2013.01.010.
23. Pu Y, Liu B, Xue G, Liang H, Ma F, Yang M, et al. Carbon/Basalt Fibers Hybrid Composites: Hybrid Design and the Application in Automobile Engine Hood. *Polymers* **2022**, *14*, 3917.

24. Azimpour-Shishevan F, Akbulut H, Mohtadi-Bonab MA. Mechanical and Thermal Properties of Carbon/Basalt Intra-ply Hybrid Composites. I. Effect of Intra-ply Hybridization. *Fibers Polym.* **2020**, *21*, 2579–2589. doi:10.1007/s12221-020-9843-6.

25. Kuciel S, Mazur KE, Robakowska M, Paukszta D. Mechanical, Thermal and Performance Evaluation of Hybrid Basalt/Carbon Fibers Reinforced Bio-Based Polyethylene Terephthalate (BioPet) Composites. *Int. J. Precis. Eng. Manuf. -Green Technol.* **2024**, *11*, 1557–1573. doi:10.1007/s40684-024-00616-w.

26. Fidan S, Özsoy Mİ, Bora MÖ, Ürgün S. Advanced hybrid composites: A comparative study of glass and basalt fiber reinforcements in erosive environments. *Polym. Compos.* **2024**, *45*, 12071–12091. doi:10.1002/pc.28619.

27. Balasubramanian B, Chandrasekar M, Chinnasamy R, Thiagamani SMK, Krishnasamy S, Dhandapani A. Quasi-Static Indentation Response of the Glass/Basalt Fibre Reinforced Hybrid Composites. *Mater. Circ. Econ.* **2024**, *6*, 38. doi:10.1007/s42824-024-00130-z.

28. Natarajan E, Mozhuguan Sekar S, Markandan K, Ang CK, Franz G. Tailoring Basalt Fibers and E-Glass Fibers as Reinforcements for Increased Impact Resistance. *J. Compos. Sci.* **2024**, *8*, 137.

29. Raajeshkrishna C, Chandramohan P, Saravanan D. Effect of surface treatment and stacking sequence on mechanical properties of basalt/glass epoxy composites. *Polym. Polym. Compos.* **2019**, *27*, 201–214. doi:10.1177/0967391118822273.

30. Arceo A. Comparative Sustainability Assessment of Decentralised Power Supply Systems in Remote Areas. Doctoral dissertation, Curtin University, Perth, Australia, 2018.

31. Wijerathne Jayawardane HT. Eco-Efficiency Performance Comparison of Additive and Subtractive Manufactured Parts. Doctoral dissertation, Curtin University, Perth, Australia, 2023.

32. Saling P, Kicherer A, Dittrich-Krämer B, Wittlinger R, Zombik W, Schmidt I, et al. Eco-efficiency analysis by basf: the method. *Int. J. Life Cycle Assess.* **2002**, *7*, 203–218. doi:10.1007/BF02978875.

33. Circle E. Sustainability Guide. Available online: https://sustainabilityguide.eu/methods/cradle-to-cradle/ (accessed on 20 September 2024).

34. Dong C. Multi-objective optimal design for carbon and basalt fibre-reinforced hybrid composites under flexural loading. *Hybrid Adv.* **2023**, *4*, 100106. doi:10.1016/j.hybadv.2023.100106.

35. Kalantari M, Dong C, Davies IJ. Multi-objective robust optimisation of unidirectional carbon/glass fibre reinforced hybrid composites under flexural loading. *Compos. Struct.* **2016**, *138*, 264–275. doi:10.1016/j.compstruct.2015.11.034.

36. Gurit. Guide to Composites. Available online: https://www.gurit.com/wp-content/uploads/2022/12/guide-to-composites-1.pdf (accessed on 24 March 2024).

37. Dong C. Flexural properties of symmetric carbon and glass fibre reinforced hybrid composite laminates. *Compos. Part C Open Access* **2020**, *3*, 100047. doi:10.1016/j.jcomc.2020.100047.

38. Kicherer A, Schaltegger S, Tschochohei H, Pozo BF. Eco-efficiency. *Int. J. Life Cycle Assess.* **2007**, *12*, 537–543. doi:10.1065/lca2007.01.305.

39. *ISO-14040*; Environmental Management—Life Cycle Assessment—Principles and Framework. International Standards Organisation: Geneva, Switzerland, 2006.

40. Renouf M, Grant T, Sevenster M, Logie J, Ridoutt B, Ximenes F, et al. *Best Practice Guide for Life Cycle Impact Assessment (LCIA) in Australia*; Australian Life Cycle Assessment Society: Fort Lauderdale, FL, USA, 2015.

41. Rudawska A, Sarna-Boś K, Rudawska A, Olewnik-Kruszkowska E, Frigione M. Biological Effects and Toxicity of Compounds Based on Cured Epoxy Resins. *Polymers* **2022**, *14*, 4915.

42. Colangelo S. Reducing the environmental footprint of glass manufacturing. *Int. J. Appl. Glass Sci.* **2024**, *15*, 350–366. doi:10.1111/ijag.16674.

43. Kawajiri K, Sakamoto K. Environmental impact of carbon fibers fabricated by an innovative manufacturing process on life cycle greenhouse gas emissions. *Sustain. Mater. Technol.* **2022**, *31*, e00365. doi:10.1016/j.susmat.2021.e00365.

44. Mohammed F, Biswas WK, Yao H, Tadé M. Identification of an environmentally friendly symbiotic process for the reuse of industrial byproduct—an LCA perspective. *J. Clean. Prod.* **2016**, *112*, 3376–3387. doi:10.1016/j.jclepro.2015.09.104.

45. Arceo A, Biswas WK, John M. Eco-efficiency improvement of Western Australian remote area power supply. *J. Clean. Prod.* **2019**, *230*, 820–834. doi:10.1016/j.jclepro.2019.05.106.

46. Yoshida H, Christensen TH, Scheutz C. Life cycle assessment of sewage sludge management: A review. *Waste Manag. Res.* **2013**, *31*, 1083–1101. doi:10.1177/0734242x13504446.

47. Kalantari M, Dong C, Davies IJ. Multi-objective robust optimization of multi-directional carbon/glass fibre-reinforced hybrid composites with manufacture related uncertainties under flexural loading. *Compos. Struct.* **2017**, *182*, 132–142. doi:10.1016/j.compstruct.2017.09.019.